APPLYING TRANSFER LEARNING BASED DEEP MODELS ON STRUCTURAL AND FUNCTIONAL BRAIN IMAGES TO PREDICT ALZHEIMER'S DISEASE

LILIA LAZLI

Department of Computer and Software Engineering, Polytechnique Montréal, University of Montreal, Canada
E-MAIL: lazlilia28@gmail.com

Abstract:

Alzheimer's disease (AD) destroys brain cells and can even cause death in older people. Therefore, diagnosis in the early stages is essential for proper treatment. Computer-aided diagnosis based on machine learning has become an accessible and suitable tool. However, the majority of traditional models focus on binary classification and utilize multi-step architectures, which are intricate and heavily reliant on human experts. This paper presents deep architectures that eliminate the need for handcrafted feature generation and significantly improve the process for accurate diagnosis. We design and train several enhanced convolutional neural networks (CNNs) based on transfer learning (TL) using smaller datasets to analyze neuroimaging scans and classify them into different AD stages. These CNNs are tested on the ADNI and OASIS benchmark datasets and found to outperform the best TL methods with regard to accuracy, precision, recall, f1-score and area under the ROC curve. The results show that NASNetLarge achieves finest performance, outperforming comparative models such as NASNet-Mobile, Inception-ResNetV2, and InceptionV3.

Keywords:

Deep learning; Computer-aided diagnosis system; CNNs architectures; Brain images processing; Alzheimer's disease

1. Introduction

Alzheimer's disease (AD) is a growing and deadly neurological disorder. Eventually, AD demolish the part of the brain that manages cardiac and respiratory functions, which leads to death. The symptoms are not visible for years until the patient reaches an advanced stage. Thus, diagnosis of AD at an early stage contributes to appropriate treatment and prevention of brain tissue damage.

Computer-aided diagnosis (CAD) based on artificial intelligence (AI) has become an accessible and suitable tool in medicine owing to its translucent decision-making and reasonable cost. Despite distinguishing AD, it stays an ambitious task in computer vision areas, but the AI sub-branch of machine learning (ML) offers techniques that can significantly improve the process of obtaining accurate information for AD diagnosis. However, most CAD systems in the literature are based on multi-step architectures, which are hard and greatly controlled by human experts. Besides, these systems are designed for binary classification.

To tell the difference between healthy controls (HC) and people in different early stages of AD, we need new models that are based on deep knowledge and a lot of experience.

This paper presents an effective automated CAD system based on robust deep learning (DL) architectures. The following are our primary contributions: (1) We started with the idea that it was vital to create architectures capable of training useful features from small neuroimaging databases. To achieve this, we used newer convolutional neural networks (CNNs) architectures, which are efficient in transfer learning (TL) and allow faster training of models. (2) We designed the pretrained models InceptionV3 [1], Inception-RestNetV2 [2], as well as NASNet-Mobile and NASNetLarge [3], trained on the ImageNet dataset [4], to analyze the two neuroimages commonly used in AD diagnosis, namely structural magnetic resonance imaging (sMRI) and fluorodeoxyglucose positron emission tomography (FDG-PET). (3) The most challenging datasets, Alzheimer's Disease Neuroimaging Initiative (ADNI) and Open Access Series of Imaging Studies (OASIS), undergo rigorous tests using various experimental settings. (4) We propose CNN models to classify brain images into three major stages for ADNI: HC, mild cognitive impairment (MCI), and AD, and into four stages for OASIS: HC, very mild impairment (eMCI), MCI, and moderate (AD).

The the paper is structured as follows: In Section 2, related works are presented in brief. Section 3 summarizes deep CNN architectures, while Section 4 describes validation studies to assess the efficiency of the proposed model. Section 5 gives closing remarks and forthcoming experience.

2. Related work

Scientists have developed various CAD systems for precise AD diagnosis using conventional ML and DL models. Aversen et al. [5] analyzed sMRI data using dimensional reduction and variation methods. The researchers have utilized binary and multi-class classifiers based on support vector machines to distinguish AD images from the ADNI database. Hybrid DL architecture was established for the early-stages diagnosis of AD [6], and enhanced CNNs were presented for AD diagnosis applying multimodal neuroimaging data [7]. Yu et al. proposed a generative adversarial network based on semi-supervised learning, tensor-train, and high-order pooling [8]. Several scientists have developed CNN architectures for feature extraction and used conventional ML models for AD classification [9]. Moreover, a 3D-CNN architecture was used jointly with MRI data [10]. A multi-instance DL architecture based on dual-attention was proposed for local and global feature extraction and then to develop a CAD system [11]. Finally, a Monte Carlo ensemble artificial neural network was developed for AD diagnosis using 2D images from various datasets [12].

Medical image data provides feature vectors for training conventional ML models. Human experts are required to extract the features, which often requires a significant investment of time, labor and funds. With the progress of DL framework, it is now possible to perform a feature extraction just from the images without human intervention. Therefore scientists are concentrating on developing DL architectures for precise AD diagnosis.

DL has shown a prominent result for medical analysis, however there is modest contributions for diagnosis of AD. On the other hand, the development of robust deep neural networks requires a lot of images. Generally, neuroimaging datasets, and especially our datasets, contain fewer images for training. We leveraged the predictive capabilities of various CNN models pre-trained by transfer learning in our system. This strategy proved advantageous in overcoming the lack of sufficient image databases.

3. Material and method

3.1. Data acquisition

The experiments were performed on the sMRI and DFG-PET images acquired from the ADNI (adni.loni.usc.edu) and OASIS (oasis-brains.org). For each type of scan, we used 813 (belonging to 459 male and 354 female subjects) for the first dataset and 416 (168 male and 248 female subjects) for the second. OASIS subjects range in age from 18 to 96 years old, and the age range of the ADNI subjects was between 60 − 90 with a mean of 75.83 and a standard deviation of 6.07.

We used a clinical dementia rating (CDR) scale to control the dementia status of the dataset; a score of 0 on the scale indicates a normal cognitive level, and a score greater than 0 but less than 2 indicates mild impairment and finally, a score of 2 or higher determines moderate Alzheimer's. In this context, we split the images into 187 AD, 228 HC, and 398 MCI for ADNI, and 300 HC, 70 eMCI, 28 MCI, and 18 AD for OASIS.

Many slices of scans were collected from each subject for precise classification of different stages of the disease. The middle slices enclose further tissue than the border slices. Hence, tissues present a biomarker for dementia; central slices help the CAD system to accurately classify AD. Therefore, they are used for training. Fig.1 shows some sample images of HC and AD patients.

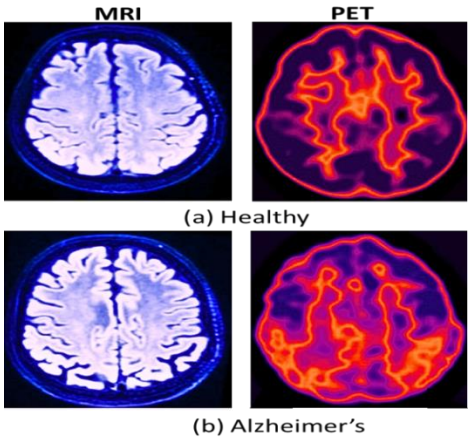

FIGURE 1. Samples of MRI and PET images: HC (top-row), AD (bottom-row)

3.2. Preprocessing

We used the statistical parametric mapping (SPM8) tool [13] to partially correct spatial intensity inhomogeneities. Origin of the raw sMRI scans was set manually to anterior commissure before manually registering them with SPM's canonical T1 template image. We applied the N3 (non-parametric non-uniform intensity normalization) technique to solve the tissue intensity non-uniformity problem [14]. Then the hybrid median filter was employed to remove impulse noise while preserving edges**.** Each slice of sMRI includes 256 × 256

× 176 voxels covering the entire region of the brain with the following parameters: Voxel size is 2 × 2 × 2 mm^3 for ADNI and 2 × 3.1 × 2 mm^3 for OASIS; Isotropic resolution is 1.0 mm; time of repetition is 5050 ms; time of echo is 10 ms. All slices of reconstructed PET images are resampled to contain 256 × 256 × 207 voxels with a voxel size of 1.2 × 1.2 × 1.2 mm^3.

3.3. Classification

We generated additional data from sMRI and FDG-PET images to train the deep models, thereby enhancing the robustness of our predictions. In this regard, data augmentation was applied to our datasets to increase the number of samples in the training dataset to avoid overfitting in CNN networks. We mainly achieved the augmentation by flipping the images horizontally, rotating them by a certain degree, rescaling (resizing) them in the range of [0, 1], and applying min-max normalization.

We used CNN models, already trained with TL, to classify people at different stages of AD. Our datasets could thus exploit the knowledge of ImageNet [4]. We pass the pre-processed images to each pre-trained model, which transforms each input into an output with building a hierarchy of features starting with simple low-level features and going to complex high-level features. As network architectures, we applied InceptionV3 [1]and Inception-RestNetV2 [2] as well as two variants of NASNet architecture [3] based on reinforcement learning and recurrent network which are NASNet-Mobile, and NASNetLarge.

TABLE 1. The hyperparameters of the four CNNs used for the experiment

Neural network	Depth	Size	Param	Image Size
InceptionV3	48	89 MB	23.9	299-by-299
Inception-ResNetV2	164	209 MB	55.9	299-by-299
NASNet-Mobile	*	20 MB	5.3	224-by-224
NASNetLarge	*	332 MB	88.9	331-by-331

* The NASNet-Mobile and NASNetLarge CNNs do not consist of a linear sequence of modules.

For the first CNN model, we provide obvious empirical evidence that training with residual connections expedites the training of Inception CNN considerably. The second network is developed using the original baseline weights of ImageNet dataset and entirely fine-tuning all network layers to estimate the root mean square error and inference time for prediction. Data, using a recurrent neural network, informed the latest two models, unlike other pre-trained models entirely designed by humans. The hyperparameters of each CNN are presented in Table 1.

Each architecture has many layers which achieve four fundamental operations: convolution, batch normalization, rectified linear unit, and pooling. The network layers track a specific connection pattern namely dense connectivity, where each layer is connected to every other layer. The final classification is performed via a softmax layer which contains three (ADNI samples) or four (OASIS samples) different output classes.

The CNN model takes an MRI or PET image as input and generates the corresponding learned features. This allows the image to be classified into one of the network's output classes. We applied cross entropy loss function to estimate the loss of each network. The learned features, f_i are considered by the Softmax layer which transliterates them to the output class. Furthermore, a probability score s_i is entrusted to the output class whose formula as follows.

$$s_i = exp(f_i) \Big/ \sum_{i=1}^{n} exp(f_i) \tag{1}$$

$$\epsilon = -\sum_{i=1}^{n} g_i log(s_i) \tag{2}$$

where n is the number of AD stages and ϵ is the loss of cross entropy of the network. Back propagation is used to calculate the gradients of the network. If the ground truth of an input image is denoted as g_i, then:

$$\partial\epsilon/\partial f_i = s_i - g_i \tag{3}$$

5-fold cross validation is performed since the dataset is small. For each fold, a split ratio of 70:30 was used for the training and test sets. We took 10% data from the training dataset to produce the validation dataset. Test data were used to measure the model's behavior with previously unseen data. This makes it possible to evaluate the goodness of the trained CNN models in order to improve them. We optimize the models using the stochastic gradient descent algorithm and use early-stopping for regularization.

4. Results

We used the statistical indices, namely true positives, false positives, false negatives, and true negatives, to compute five

performance metrics for quantitative evaluation, including accuracy (Acc), precision (Prc), recall (Rec), f1-score (F1), and area under the ROC curve (Auc) score. Figures 2 to 5 present the classification performances of the four proposed models on ADNI and OASIS datasets for sMRI and FDG-PET images, respectively.

The NASNetLarge CNN achieves finest performance for classifying different stages of AD compared to other models. This model works very well to classify both MRI and PET neuroimaging data. For ADNI images, the performances in term of accuracy are: MRI (90.8, 85.3, 94.3) % and PET (91.6, 80.5, 90.3) % for AD, MCI and HC stages respectively. The same finding for OASIS images, the Accuracy results are: MRI (96.5, 88.6, 85.7, 97.2) % and PET (91, 85.3, 84.1, 90.2) % for AD, MCI, eMCI, and HC stages respectively. Figures 6 and 7 present ROC curves obtained with the DL classifiers for the multi-class classification of all stages.

The results obtained are statistically significant with a p-value of 0.019, lower than the alpha significance threshold (confidence level). This ensures the significant difference between patients with AD and healthy subjects.

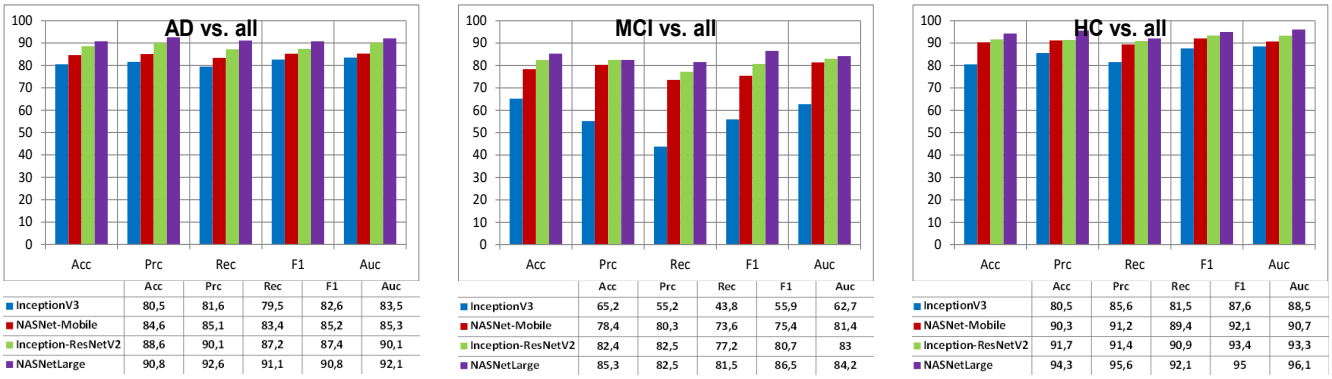

FIGURE 2. Multi-class classification performance for sMRI test data from ADNI dataset

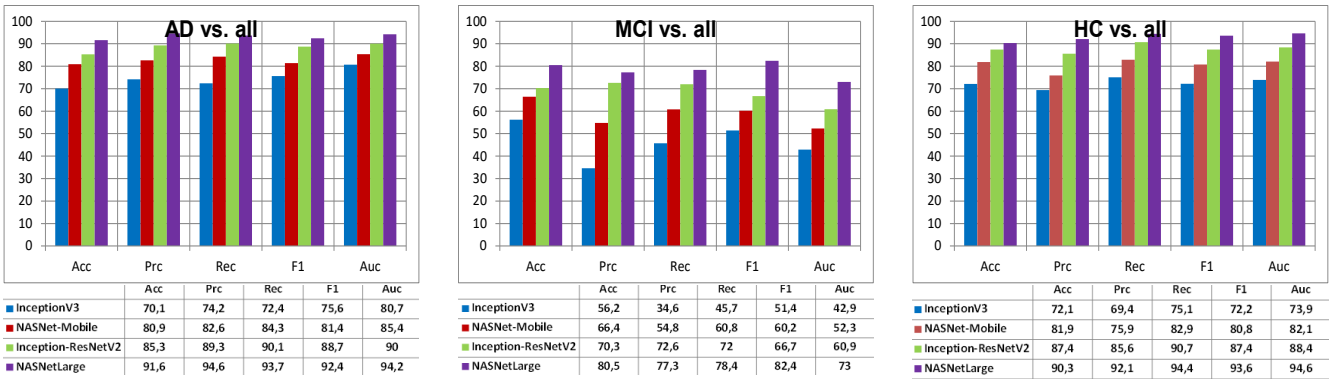

FIGURE 3. Multi-class classification performance for FDG-PET test data from ADNI dataset

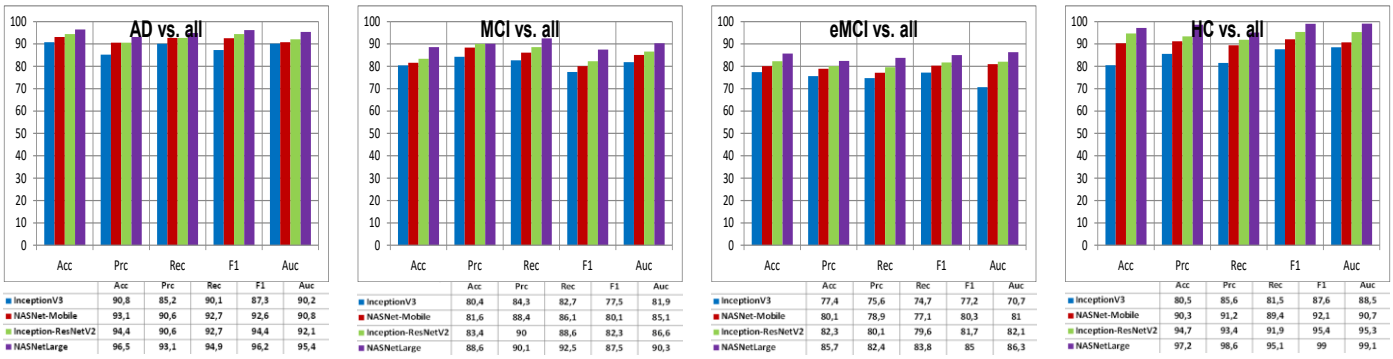

FIGURE 4. Multi-class classification performance for sMRI test data from OASIS dataset

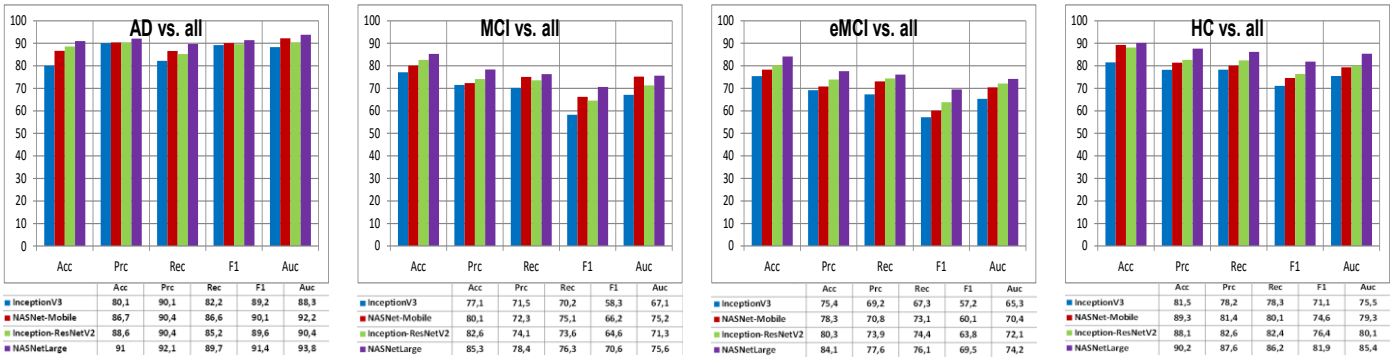

FIGURE 5. Multi-class classification performance for FDG-PET test data from OASIS dataset

Thus, although this type of network provided adequate performance for the classification of non-demented and AD stages, there is still much to be done to improve the diagnosis of patients with very mild or mild impairment. To overcome this limitation, it will be reasonable to train CNN with a dataset that contains more samples of patients with dementia.

Inception-RestNetV2 and NASNet-Mobile have already demonstrated outstanding performance in comparison with the InceptionV3 baseline model. Nevertheless because of the lack of sufficient training data, both CNNs suffered overfitting which caused a performance degradation in classifying different AD stages.

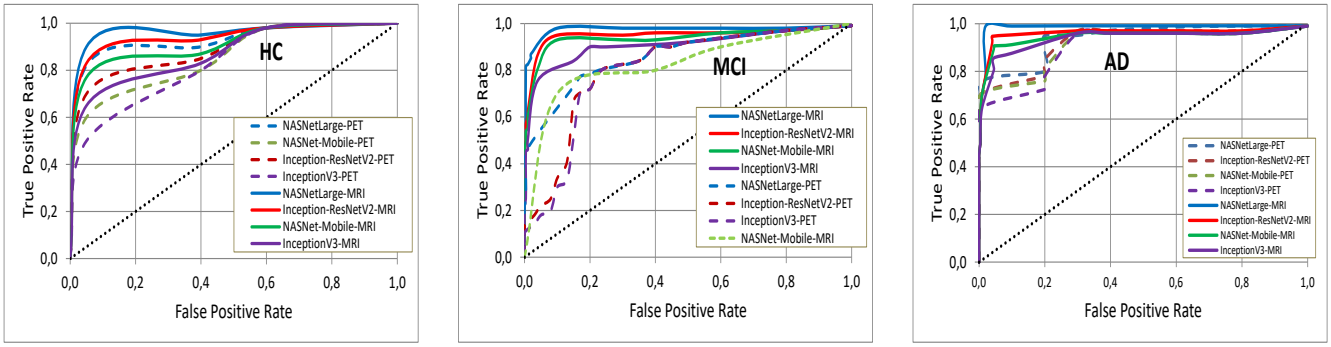

FIGURE 6. ROC curves obtained with DL classifiers for ADNI multi-class classification of HC, MCI, and AD stages

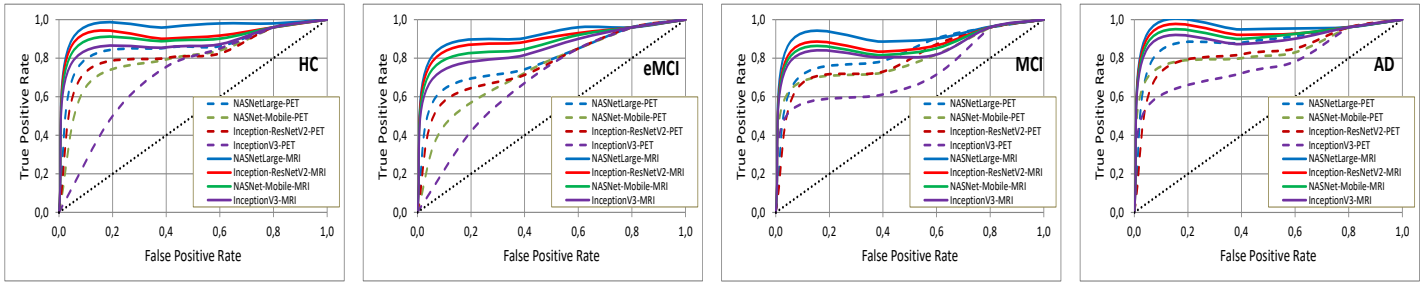

FIGURE 7. ROC curves obtained with DL classifiers for OASIS multi-class classification of HC, eMCI, MCI, and AD stages

5. Conclusion

A CAD system is decisive for the early diagnosis of AD and thus for planning the appropriate treatment for patients suffering from this disease. In this paper, some recent and improved pre-trained CNNs based on TL are designed and trained with smaller datasets to analyze neuroimaging scans. The suggested CNN models can identify early stages of AD and favourably classify sMRI and FDG-PET images from OASIS and ADNI challenging datasets into different stages.

We demonstrated that using hyper-parameters from a very deep image classifier pre-trained with ImageNet can aid feature learning from small dataset. In this context, NASNetLarge performed better than the baseline models Inception-ResNetV2, NASNet-Mobile, and InceptionV3. The application of transfer learning enabled this network to handle small-scale medical data well. In addition, the joint use of MRI and PET brain images, as well as the comparative evaluation of some of the most popular deep models currently available, improves the strength and generalizability of finding.

Whereas most existing studies focuses on binary classification, the proposed CNN architectures provided significant enhancement to multi-class classification. We tested the proposed models only on AD datasets, but we believe they can successfully address other classification problems in the medical domain.

Acknowledgments

This project was supported by the “Fonds de recherche du Québec-Nature et Technologies –FRQNT” grants under award numbers 255325 (https://doi.org/10.69777/255325) and 358107 (https://doi.org/10.69777/358107).

The OASIS-3 data were provided in part by OASIS Longitudinal Multimodal Neuroimaging: Principal Investigators: T. Benzinger, D. Marcus, J. Morris; NIH P30 AG066444, P50 AG00561, P30 NS09857781, P01 AG026276, P01 AG003991, R01 AG043434, UL1 TR000448, R01 EB009352. Data collection and sharing for ADNI was funded by the Alzheimer’s Disease Neuroimaging Initiative (ADNI) (National Institutes of Health Grant U01 AG024904) and DOD ADNI (Department of Defense award number W81XWH-12-2-0012).

Availability of data and materials

The datasets were obtained from the Alzheimer’s Disease Neuroimaging Initiative (adni.loni.usc.edu) and the Open Access Series of Imaging Studies (oasis-brains.org). The source code can be accessed at: github.com/Lilaz28/NASNetLarge

References

[1] Szegedy. C., Vanhoucke. V., Ioffe. S., Shlens. J., & Wojna. Z., “Rethinking the Inception Architecture for Computer Vision”, IEEE Conference on Computer Vision and Pattern Recognition, pp. 2818-2826, 2016.

[2] Szegedy., C., Ioffe. S., Vanhoucke. V., & Alemi. A-A., “Inception-v4, inception-ResNet and the impact of residual connections on learning”, Proceedings of the Thirty-First AAAI Conference on Artificial Intelligence, pp. 278-4284, 2017.

[3] Barret. Z., Vasudevan. V., Shlens. J., & Quoc V. Le. Q-V., “Learning Transferable Architectures for Scalable Image Recognition”, IEEE/CVF Conference Computer Vision and Pattern Recognition, pp. 8697- 8710, 2018.

[4] ImageNet, http://www.image-net.org, last accessed 2023/02/16.

[5] Arvesen. E., “Automatic classification of Alzheimer’s disease from structural MRI”, Master’s thesis, 2015.

[6] Balaji. P., Chaurasia. M-A., Bilfaqih. S-M., Muniasamy. A., Alsid. L-E-G., "Hybridized Deep Learning Approach for Detecting Alzheimer's Disease", Biomedicines, 11, 149, 2023.

[7] Pei. Z., Wan. Z., Zhang. Y., Wang. M., Leng. C., Yang. Y-H., "Multi-Scale Attention-Based Pseudo-3D Convolution Neural Network for Alzheimer's Disease Diagnosis Using Structural MRI", Pattern Recognition, 131, 108825, 2022.

[8] Yu. W., Lei. B. Ng. M-K., Cheung. A-C., Shen. Y., Wang. S., "Tensorizing GAN With High-Order Pooling for Alzheimer's Disease Assessment", IEEE Trans. Neural Netw. Learn. Syst., 33, pp. 4945–4959, 2022.

[9] Zhang. X., Yao. L., Wang. X., Monaghan. J., McAlpine. D., Zhang. Y., "A Survey on Deep Learning-Based Non-Invasive Brain Signals: Recent Advances and New Frontiers", J. Neural Eng., 18, 031002, 2021.

[10] Feng. W., Van Halm-Lutterodt. N., Tang. H., Mecum. A., Mesregah. M.K., Ma. Y., Li. H., Zhang. F., Wu. Z., Yao. E., et al., "Automated MRI-Based Deep Learning Model for Detection of Alzheimer's Disease Process", Int. J. Neural Syst., 30, 2050032, 2020.

[11] Zhu. W., Sun. L., Huang. J., Han. L., Zhang. D., "Dual Attention Multi-Instance Deep Learning for Alzheimer's Disease Diagnosis With Structural MRI", IEEE Trans. Med. Imaging, 40, pp. 2354–2366, 2021.

[12] Liu. C., Huang. F., Qiu. A., "Monte Carlo Ensemble Neural Network for the Diagnosis of Alzheimer's Disease", Neural Netw., 159, pp. 14–24, 2023.

[13] spm8. Available online: https://www.fil.ion.ucl.ac.uk/spm/software/spm8/ (accessed on 20 october 2022).

[14] N3. Available online: http://www.bic.mni.mcgill.ca/software/N3/ (accessed on 23 October 2022).